Received: 24 April 2019 | Revised: 23 September 2019 | Accepted: 27 October 2019

DOI: 10.1111/coin.12259

SPECIAL ISSUE ARTICLE

Computational Intelligence WILEY

Brain tumor diagnosis based on artificial neural network and a chaos whale optimization algorithm

Shu Gong[1] | **Wei Gao**[2] | **Francis Abza**[3]

[1]Department of Computer Science, Guangdong University Science and Technology, Dongguan, China

[2]School of Information Science and Technology, Yunnan Normal University, Kunming, China

[3]Department of Computer Science, University of Ghana, Legon-Accra, Ghana

Correspondence
Shu Gong, Department of Computer Science, Guangdong University Science and Technology, Dongguan, China.
Email: gongshu_gk@126.com

Abstract

Accurate and early detection of the brain tumor region has a great impact on the choice of treatment, its success rate, and the follow-up of the disease process over time. This study presents a new bioinspired technique for the early detection of the brain tumor area to improve the chance of completely healing. The study presents a multistep technique to detect the brain tumor area. Herein, after image preprocessing and image feature extraction, an artificial neural network is used to determine the tumor area in the image. The method is based on using an improved version of the whale optimization algorithm for optimal selection of the features and optimizing the artificial neural network weights for classification. Simulation results of the proposed method are applied to FLAIR, T1, and T2 datasets and are compared with different algorithms. Three performance indexes including correct detection rate, false acceptance rate, and false rejection rate are selected for the system performance analysis. Final results showed the superiority of the proposed method toward the other similar methods.

KEYWORDS

artificial neural network, brain tumor, feature classification, tumor detection, whale optimization algorithm

1 INTRODUCTION

A brain tumor is a type of hard neoplasm inside the brain and central canal of the spinal cord. In simpler terms, a brain tumor is an abnormal mass in the brain that may be malignant (cancerous) or benign (noncancerous) nature.

The extent of a tumor's threat depends on a variety of factors such as its type, location, size, life span, and how it spreads and develops. The brain is completely covered by the skull.[1-3]

This enables the early detection of brain tumors only if there are a preclinical device and appropriate diagnostic tools to assess intracranial cavity status in the early stages of tumor formation. Even with these tools, it is very difficult to accurately diagnose brain tumors due to their variety in shape, size, and appearance. In addition, in most cases, brain tumors are diagnosed in advanced stages of the disease and their occurrence may lead to unexplained signs and symptoms in the patient.[4-6]

Magnetic resonance imaging (MRI) is typically used to visualize details of the internal structure of the body. In this imaging method, the difference in magnetic properties of the textures is used to form the image.[4]

Magnetic moment of core for some elements is exposed to strong magnetic fields along with it. The amplitude of the received signal is quite simple in the MRI of two factors: the proton density and the T1 and T2 contact times.

The T1 rest time is the time interval in which 63% of the longitudinal magnetic moment of a proton moves from the perpendicular direction to the parallel direction of the field after excitation. The T2 charge period is the period of time that the transverse magnetic field of a proton decreases by about 37% of its initial value.

The pathological processes increase the T1 and T2 intercalation times and compare with the natural texture of the surroundings in the T1-weighted low-signal domain darker (and in the T2-weighted image-domain) image.

According to the aforementioned explanations, it is possible to diagnose the brain tumors with image processing in terms of uniformity of brightness intensity.[7] Manually separating the tumor region in brain, MRI is a complex and quite difficult process.

Nowadays, with the advancement of image processing algorithms, it has been possible to diagnose the brain tumors automatically. Automated methods of brain tumor detection, despite the fact that they reduce operator work and human error, make it easy to store tumor growth status over the long term.

In recent years, using computer-assisted diagnostic (CAD) systems for helping clinicians to the diagnosis of diseases and abnormalities like brain tumor in the body is increasing.[8,9] Despite several works have been done for the brain tumor detection, most of them fail in precise detect if tumor area due to the presence of the noise in the input images. This shortcoming overlaps the intensity distribution and the texture distribution of the healthy areas and tumors. This reason leads researchers to work more about improving the CAD diagnosis systems.[10]

Three main steps for tumor detection based on image processing are preprocessing, image segmentation, image feature extraction, and finally image classification based on the achieved features[11-13] (Figure 1).

In order to promote the quality of the input medical images due to their widespread, image preprocessing has been utilized. This operation is an important part of image processing that attempts to clarify the brain tissue details along with decreasing the impact of noise. The proper

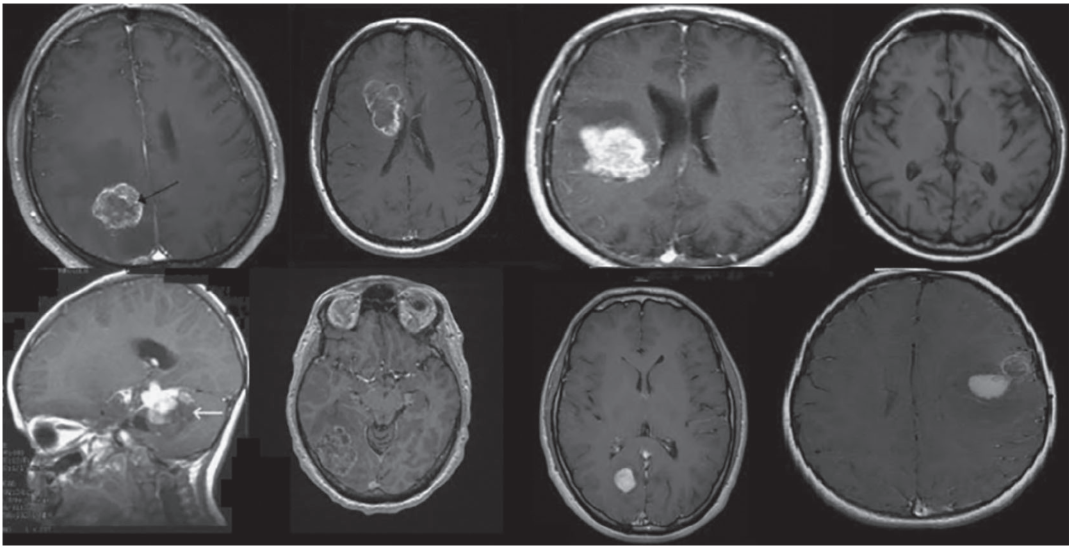

FIGURE 1 Some samples of brain tumor dermoscopic images[1]

preprocessing operation helps the system to get better results in the next steps, especially image segmentation.[14-16]

The next step is image segmentation. The process of splitting the image into its components to extract the desired objects is called image segmentation. Indeed, in image segmentation, the image surface is divided into sections that share the same properties, do not overlap, and assemble all of those parts to the entire image surface using existing methods. Image segmentation is a fundamental procedure in medical image analysis to interpret those images.

Some examples are area-based and active range-based methods,[17] the threshold for illumination intensity,[18,19] unsupervised methods,[20,21] and supervised classifiers.[22,23]

Image thresholding is an applicable method for image segmentation. Image thresholding is to convert an input image to a binary image which needs to set a threshold and set all pixels below the threshold value to 0 and all pixels above the threshold value to 1 (or 255). Some examples of this technique for brain tumor detection is the threshold based on statistical information,[18] or on the basis of a map or bracket, atlas to increase accuracy,[19] and the PET-CT dual fashion method.[24]

Active contour-based methods define a curve for the detection of the studied image, and the curve interval coincides with the energy minimization process and uses the image local information to the boundaries of the target area.[17] They also used the genetic algorithm for improving the performance of the active counter methodology for increasing the tumor detector speed as a way to search the border of the tumor area.[25]

Another approach for brain tumor detection is to use artificial neural networks (ANNs).[13,23,26-28] For instance, Bayesian-based methods like Maximum A Posteriori is an applicable method for brain tumor segmentation.[29]

Using the support vector machines (SVMs) is a very convenient technique for image segmentation, including MRI images of the brain, especially when training samples includes a small number of samples and the dimensions of the feature space are very large.[30]

Another method to achieve precise and high-speed results is to use SVMs. A combination of SVM and genetic algorithm were used to improve the system segmentation accuracy.[31]

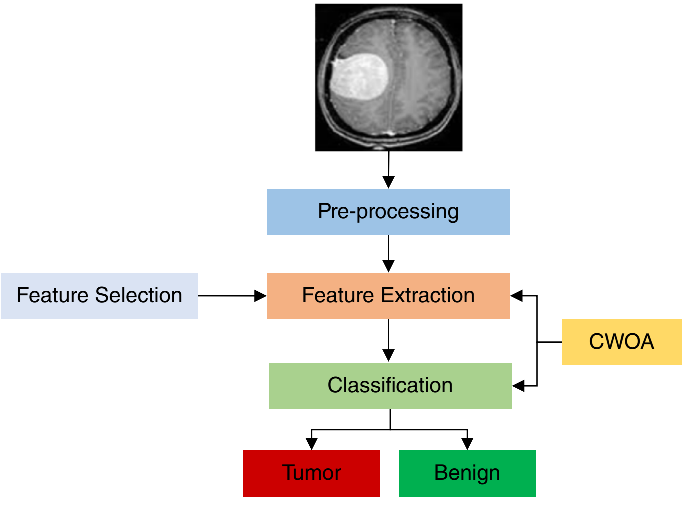

FIGURE 2 Flowchart diagram of the proposed technique [Color figure can be viewed at wileyonlinelibrary.com]

Another method for the diagnosis of a brain tumor is to use the decision tree.[31] As before said, unsupervised (clustering) methods also can be used for this purpose. For instance, K-means is simple and easy to use a clustering method which utilizes to classify the pixels in an input image into different K classes.[32]

Another potential and powerful clustering method is C-means. There are different improved versions for this technique. The modified fuzzy C-means clustering algorithm is an example of these methods which was used for detection of the tumorigenic regions.[33]

Kekre et al proposed a combination of SOM ANNs by FCM to enhance the system detection accuracy for the brain tumors diagnosis.[34]

Kaur et al proposed a feature-based classification method for the diagnosis of cancerous medical images.[2,35] An important characteristic of a feature-based image classification method is its optimal features selection based on pruning the extra features.[36-39]

The main purpose of this paper is to use a new improved version of whale optimization algorithm (WAO) optimization for two purposes: optimal features selection and to optimal weights selection for an MLP ANN system for the final classification.

A general block diagram of the presented method is shown in Figure 2.

2 | PREPROCESSING

In medical images, there are several structures: normal and abnormal. Organs, bones, muscles, and fats are considered normal structures and tumors, wounds, injuries and fractures are considered abnormal structures. These anatomical structures are determined by the segmentation of medical images. In the following, image segmentation methodology in this study is declared.

Noise reduction is a process of eliminating noise from a signal. This signal can be an image, video, or audio file. All recording devices have features that expose them to noise. Noise can be random or white noise (a signal is said to be uniformly distributed at all frequencies as a function of its power density). Image noise can be caused by several reasons like image degradation in the measurement of the environment (eg, accidental perturbation), uneven attenuation of the sensor

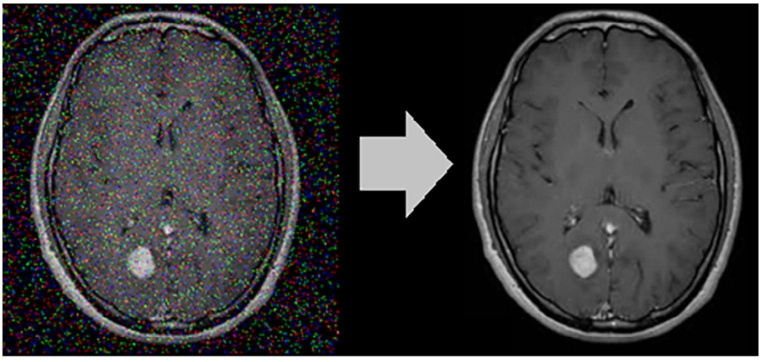

FIGURE 3 (A) Brain tumor image with salt and pepper noise by density equal to 0.08 and (B) image after noise removal [Color figure can be viewed at wileyonlinelibrary.com]

noise sensor attenuation (eg, camera movement or out of focus), exaggeration (eg, distortion), and geometric distortion (eg, earth photos taken by camera).

The purpose of removing noise from brain tumor images is to reconstruct the distorted image and restore it to its original state based on ideal models.

The most important and, of course, the most common method for noise reduction is the use of the median filter. The median filter can be used for noise reduction while keeping the image edges. In median filtering, pixels are replaced by the median value of their neighbors as follows:

$$y(i,j) = \text{med}[x(i,j) \, : \, (i,j) \in \rho], \tag{1}$$

where ρ is the neighborhood surrounding the image position (i, j).

Figure 3 shows an example of noise reduction of a brain tumor image with salt and pepper noise by density equal to 0.08 using median filter method.

The above result shows that using the median filter gives good results for the noisy tumor image.

3 | IMAGE SEGMENTATION

As mentioned earlier, image thresholding here is utilized for brain tumor images segmentation. In other words, good feature extraction will be made if the image segmentation gives good results. In this research, the Otsu method is adopted for thresholding. The method searches for a threshold level to minimize the image variance that is formulated as follows:

$$\sigma_\rho^2(t) = \rho_1(t)\sigma_1^2(t) + \rho_2(t)\sigma_2^2(t), \tag{2}$$

where ρ_i describes the probability for two separate classes with a threshold value of t and σ_i^2 describes the variance for each class.

The method is a kind of minimization technique for the class-like variance value for maximizing the class-in-variance.

$$\sigma_\omega^2(t) = \sigma^2 - \sigma_\rho^2(t) = \rho_1(t)\rho_2(t)[\mu_1(t) + \mu_2(t)]^2, \tag{3}$$

where $\mu_i(t)$ describes the mean value and has been updated continuously.

In Otsu's method, after evaluating the histogram of the intensity levels, it initializes the values of $\rho_i(0)$and $\mu_i(0)$ to all possible threshold levels. Then, the values of $\rho_i(t)$ and $\mu_i(t)$ are updated and the optimal threshold in maximum $\sigma_\rho^2(t)$ is achieved for thresholding operation.

Afterward, morphological operations containing filling holes, opening and closing are adopted for eliminating the additional parts of the brain tumor.[40]

To fill the empty holes of the image, the following formulation has been employed:

$$F_k = (F_{k-1} \ominus se) \cap S^c, k = 1, 2, \dots, \tag{4}$$

where S and se describe the area and the structure element, respectively.

Here, a 5×5 identity matrix is employed as the structural element.

Afterward, the morphology opening is performed to eliminate the lighter details with keeping other gray surfaces. This operation is formulated as follows:

$$F \odot se = (F \ominus se) \oplus se. \tag{5}$$

Finally, morphological closing is applied to connect the narrow parts of the processed image. The equation for closing is given in the following:

$$F \odot se = (F \oplus se) \ominus se. \tag{6}$$

Figure 4 shows some samples of brain tumor segmentation based on the proposed method.

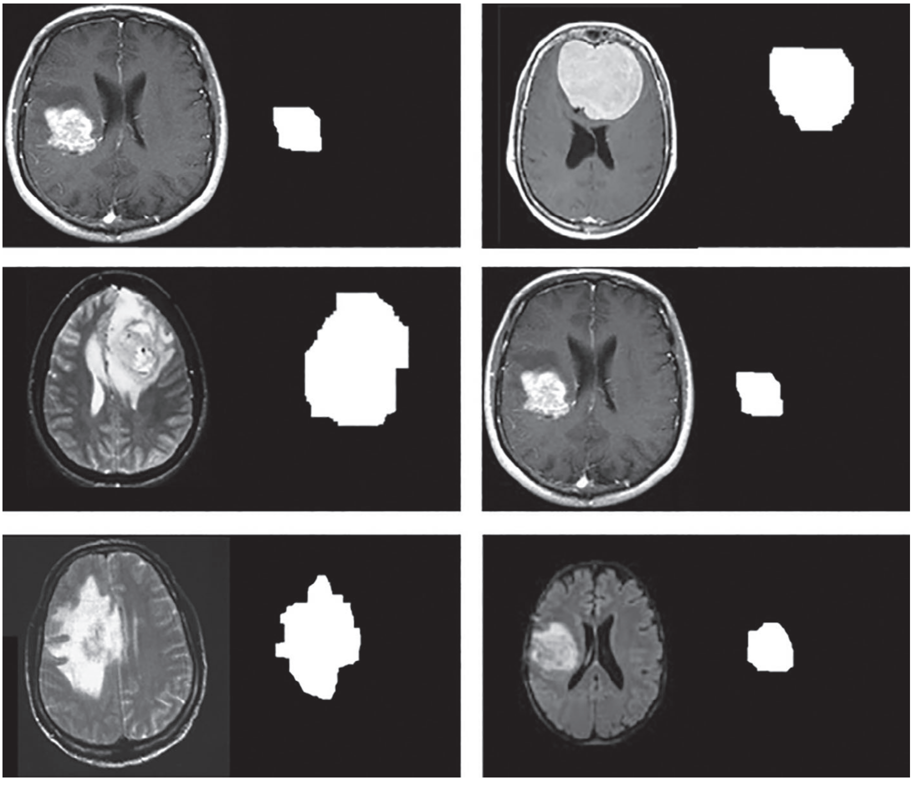

FIGURE 4 Some examples of brain tumor detection

4 | WAO BASED ON CHAOS THEORY

4.1 | The original WAO

One of the largest rorqual species whales is the humpback whale. An adult humpback whale is about the size of a school bus. Their favorite hunt is small fish groups. The most interesting thing about humpback whales is the specific way they are hunted. This exploratory behavior is known as the bubble feeding method. Humpback whales prefer to hunt bunches of small creatures or fish near the water's surface. It has been observed that this exploration is accomplished by generating index bubbles along a circle or paths.[41-43]

The WOA algorithm is one of the nature-inspired optimization algorithms which is inspired from the bubble net hunting process of the humpback whales and can be used in different optimization problems.[44-46]

The algorithm starts with a random vector of variables as the whale's population to find the global solution for the optimization problem. The bubble-net feeding process of the humpback whale is A mathematically modeled as follows:

$$Z(t+1) = \begin{cases} Z^*(t) - AD, & p < .5 \\ D'e^{bl}\cos(2\pi t) + Z^*(t), & p \geq .5. \end{cases} \tag{7}$$

$$D' = |CZ^*(t) - Z(t)|. \tag{8}$$

$$A = 2ar - a. \tag{9}$$

$$C = 2r. \tag{10}$$

where l represents a random variable between -1 and 1, a is a descent integer from 2 to 0 linearly over the iteration, r and p describe random constants in the interval 0, 1, b defines the logarithmic shape of the spiral motion, t is the current iteration, and D' describes the distance of the ith whale from the the best solution (prey).

Here, the convergence of the method will be guaranteed if $|Z| > 1$. the algorithm exploration is improvement by the following formula:

$$D' = |CZ_{\text{rand}}(t) - Z(t)|. \tag{11}$$

$$Z(t+1) = \begin{cases} Z_{\text{rand}}(t) - AD, & p < 0.5 \\ D'e^{bl}\cos(2\pi t) + Z_{\text{rand}}(t), & p \geq 0.5 \end{cases}. \tag{12}$$

The main motivation of using the WAO is that although it is a new optimization algorithm, it has been used for different applications due to its good exploration capability. One problem of the WAO is that it has high complexity in converging. So, in this paper, an improved version of this algorithm is introduced to cover this shortcoming.

4.2 | WAO based on chaos theory (CWOA)

Chaos theory has been the subject of scientific research in various fields such as physics and mathematics in recent decades, but its simple meaning is rooted in human early perceptions of the universe. From the point of view of chaos theory, complex systems have a purely turbulent appearance and, as a result, appear irregular and random, while they may be subordinate to a given process with a specific mathematical formula.[47,48] A simple formulation for the chaos behavior is illustrated below:

$$\mathrm{CM}^{j}_{i+1} = f(\mathrm{CM}^{j}_{i}), \quad j = 1, 2, \dots, k, \tag{13}$$

where k describes the map dimension and $f(\mathrm{CM}^{j}_{i})$ represents to the chaotic model generator function.

Using chaos behavior can improve the system convergence and speed which improves the population diversity to escape from the local optimum trap.[47,48] In this subsection, an improved version of the WOA is utilized based on the sinusoidal chaotic map. The presented method is called Chaotic WAO (CWOA). In the proposed CWCO algorithm, the parameter X_{rand} is modeled based on the sinusoidal chaotic map as follows:

$$X_{\mathrm{rand},k} = ap_k^2 \sin(\pi p_k),$$

$$p_0 \in [0, 1], a \in (0, 4], \tag{14}$$

where k represents the iteration number.

This improvement enhances the administratorship capability of the spiral model selection for the whale's location updating. The block diagram of the proposed optimization algorithm is shown below (Figure 5).

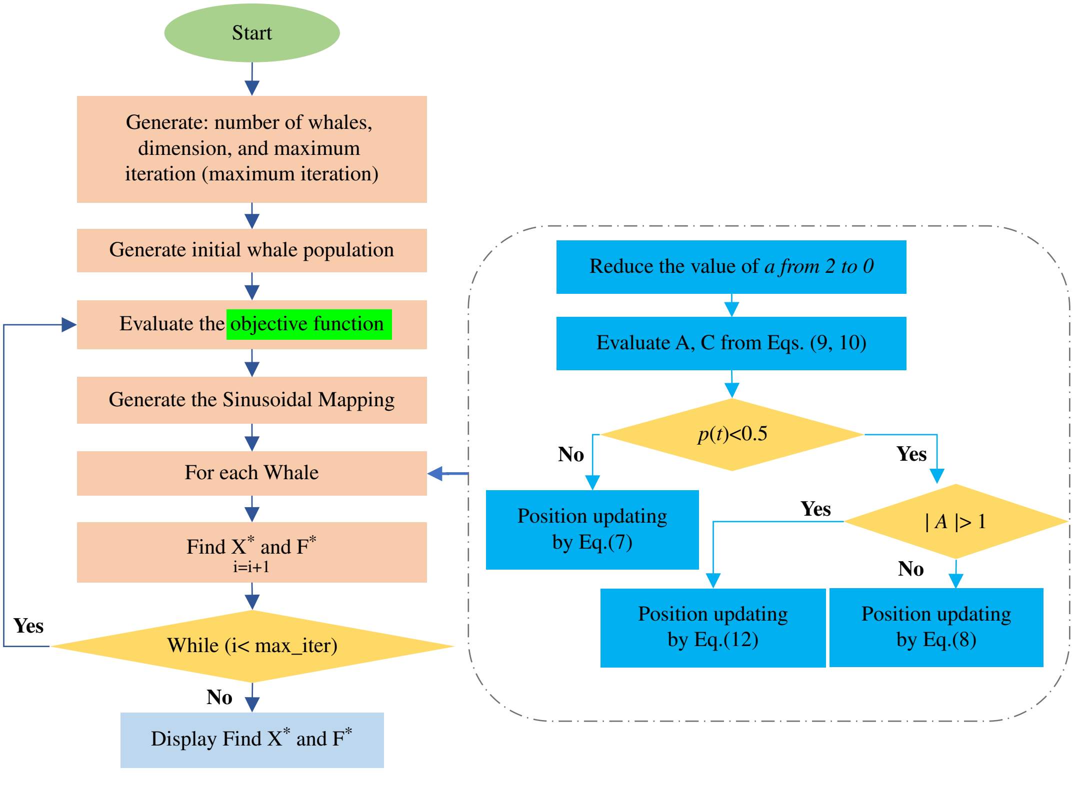

FIGURE 5 The flowchart diagram of the proposed chaos whale optimization algorithm [Color figure can be viewed at wileyonlinelibrary.com]

TABLE 1 Advantages and disadvantages of chaos whale optimization algorithm

Advantages	Disadvantage
Has higher convergence speed	Has long computational time
Can be robust	Initial value settings are required
Have higher probability and efficiency in finding the global optima	Ability to search for local is weak
Can be efficient for solving problems presenting difficulty to find accurate mathematical models	Has a high dimensional problem
Can be used for large problems	Have a difficult theoretical analysis

In Table 1 some significant advantages and disadvantages of the proposed CWAO are illustrated.

According to the results, the proposed CWAO has a simple structure and the only difference between the original WOA and the CWOA is the utilization of a logistic map for updating the algorithm. As a result, the convergence speed is improved. However, the proposed algorithm has the limitation of the high computational effort in terms of methodology and application.

5 | FEATURE EXTRACTION

Images feature extraction is one of the important operations in image processing to the comparison of content-based images. Feature extraction has been used extensively in medical imaging.[49]

In recent years, various algorithms have been proposed to image features extraction. Existing methods to extract all attribute patterns should be searched and identified. In these methods, the results are noise sensitive. Also in many of these methods, features extraction depends on

TABLE 2 Utilized features in the study

Area $= \sum_{i=1}^{M}\sum_{j=1}^{N} p(i,j)$	**Contrast** $= \sum_{i=1}^{M}\sum_{j=1}^{N} p^2(i,j)$
Rectangularity $= \frac{\text{Area}}{a\times b}$	Entropy $= -\sum_{i=1}^{M}\sum_{j=1}^{N} p(i,j)\log p(i,j)$
Perimeter $= \sum_{i=1}^{M}\sum_{j=1}^{N} b_p(i,j)$	Homogenity $= \sum_{i=1}^{M}\sum_{j=1}^{N} \frac{p(i,j)}{1+\lvert i-j\rvert}$
Elongation $= 2\times(a^{-1})\times(\pi^{-0.5})\times(\text{Area}^{0.5})$	Mean $= \frac{1}{MN}\sum_{i=1}^{M}\sum_{j=1}^{N} p(i,j)$
Variance $= \frac{1}{MN}\sum_{i=1}^{M}\sum_{j=1}^{N}[p(i,j)-\mu]$	SD $= \sqrt{\text{Variance}}$
Irregularity index $= \frac{4\pi\times\text{Area}}{\text{Perimeter}^2}$	Eccentricity $= 2a^{-1}(a^2-b^2)^{0.5}$
Form factor $= \frac{\text{Area}}{a^2}$	Energy $= \sum_{i=1}^{M}\sum_{j=1}^{N} p^2(i,j)$
Correlation $= \sum_{i=1}^{M}\sum_{j=1}^{N} \frac{p(i,j)-\mu_r\mu_c}{\sigma_r\sigma_c}$	$\phi_1 = \eta_{20}+\eta_{02}$
	$\phi_2 = (\eta_{20}+\eta_{02})^2+4\eta_{11}^2$
	$\phi_3 = (\eta_{30}-3\eta_{12})^2+(3\eta_{21}-\eta_{03})^2$
	$\phi_4 = (\eta_{30}+3\eta_{12})^2+(3\eta_{21}+\eta_{03})^2$

Abbreviations: $p(i,j)$, intensity value of the pixel at point (i,j); MN, the size of the image; μ and σ, mean and SD, respectively; b_p, the external side length of the boundary pixel; a and b, the major and the minor axis, respectively.

the complexity of the image patterns. In recent years, different types of these features have been introduced where most of them need all features to be useful.

In this study, 19 different characteristics of including texture features, statistical features, and geometric features are extracted from the segmented brain tumor. Then, the presented CWOA has been employed for optimal features selection to enhance the system efficiency by discarding similar features and pruning overfitted values. The utilized features in the paper are given in Table 2.

6 | OPTIMAL FEATURE SELECTION

Once feature selection is applied, some features are pruned and some others are kept for use in training for tumor classification. In this research, the optimal features selection is obtained by minimizing the Matthews correlation coefficient (MCC) function as the objective function and with the help of the CWOA which is explained before.[49]

The MCC is a measure for analyzing the quality of the classification in binary (two-class).[50] MCC determines the correlation between the objective and the obtained result. The coefficient switches between −1 and +1.

−1 and 1 describe a perfect disagreement and agreement between the objective and the obtained result. Here, 0 describes that the prediction may as well be random with respect to the actual. The MCC is determined by the following equation.

$$\text{Cost Function} = \frac{(\text{TP} \times \text{TN}) - (\text{FP} \times \text{FN})}{\sqrt{(\text{TN} + \text{FP}) \times (\text{TP} + \text{FP}) \times (\text{TP} + \text{FN}) \times (\text{TN} + \text{FN})}} \tag{15}$$

where TP, TN, FP, and FN are truly positive, true negative, false positive, and false negative, respectively.

So it can be mentioned that the total proposed approach contains two main parts: initializing the parameters of the WOA based on chaos theory, and then applying the presented algorithm for minimizing Equation (15) and optimal feature selection.

7 | TUMOR CLASSIFICATION BASED ON MLP-CWOA CLASSIFIER

In this section, an optimal radial basis function (RBF) network is adopted for optimal classification of the images. In this paper, CWOA is also employed to generate an optimal classifier based on the RBF network. The main idea here is to optimize the value of the RBF network weights based on the mean squared error (MSE) objective function.

ANNs are kinds of computing systems that are inspired by biological neural networks. These systems learn activities by examining examples (in other words, they improve their performance in doing activities over time), and generally, this is done without any dedicated programming.[51-55]

In the field of mathematical modeling, RBF is an ANN that uses RBFs as activation functions. The output of this network is a linear combination of RBFs for input parameters and neurons. These networks are used for approximation, time series prediction, clustering, and system control. Because RBF networks have one hidden layer, they have fast convergence speed for objective optimization. In RBF networks, the output is generated by applying a function called activation function on the input signals. The activation function of hidden neuron in RBF networks is Gaussian function which is given below:

$$\varphi(x) = e^{-\frac{(x-\mu)^2}{\sigma^2}}, \tag{16}$$

where μ and σ are the mean value and the SD of the input feature vector and $\varphi(x)$ shows the output of the Gaussian node for the given value of x.

By considering the above cases, the output layer of an RBF network performs a weighted sum of the hidden unit as follows:

$$y(t) = \sum_i \lambda_i \varphi_i(x), \tag{17}$$

where λ_i describes the ith number of the output weights.

The RBF networks evaluate the network error and then adjust the output weights to give the best output. This process is usually performed by a gradient descent algorithm which needs lots of iterations. A significant shortcoming of the gradient descent technique is that it sometimes stuck in the local minimum. This is because of its dependency on the initial weights setting.

To cover this shortcoming, a global technique is required. In this paper, the proposed CWOA is adopted instead of gradient descent to solve the aforesaid problem. Here, CWOA is adopted for optimal weights selection of the RBF networks. To do so, the MSE function is considered as the objective function.

$$\text{MSE} = \frac{1}{2} \times \sum_i \sum_j (Y_j - T_j)^2, \tag{18}$$

where i and j are the number of training samples and the number of nodes in the output, and Y_j and T_j represent the real output and the desired output, respectively. After optimizing the RBF network by the proposed CWOA, the optimal features from the previous section are assigned as the input data to the network to classify them into two classes: tumor and healthy.

8 | SIMULATION RESULTS

There are several databases for evaluating brain tumor diagnosis systems. In this study, three popular databases containing FLAIR, T1, and T2 have been employed. All the databases have 68 images, so the total number of them is 204 brain MR tumor images. Images are collected by Siemens Medical Systems.[56]

Simulation results are implemented by MATLAB R2017b platform and based on a laptop with Intel®, Core™ i7, and 16 GB RAM.

In this research, after detecting brain tumor-like areas based on simple image segmentation, 19 different features derived from three classes including statistical features, geometric features, and texture features. The features are then pruned based on the proposed optimized feature selection method based on Mathew correlation coefficients.

This function gives achieves the correlation between the TP rate and FP rate from Equation (15). This algorithm operates once the desired accuracy has been obtained.

This improves the feature selection efficiency. Afterward, the features are implemented to the designed optimized ANN for training.[57]

In this study, 85% of the data have been adopted for the training and the remained 15% have been adopted for testing. Simulation results have been compared with different state-of-the-art classification methods such as SVM-based classifier,[58] Genetic-based method,[31] particle swarm optimization algorithm,[59] particle swarm optimization-based ANN (NNPSO),[59] optimized ANN based on hybrid particle swarm optimization algorithm and biogeography-based optimization (MLPPSOBBO),[60] and ANN based on deep learning (CNN).[61]

Three different classes of the approaches are utilized here for the system analysis. The first group includes the ANN (here SVM and convolutional neural network). The second group includes the meta-heuristic-based methods including genetic algorithm,[62] particle swarm optimization algorithm, and the last group is about the combination of the ANNs and optimization algorithms including NNPSO and MLPPSOBBO, and the proposed method.

The similarity of the proposed methods is unlike the classic methods, all of the analyzed methods have simpler and easier methods for solving the problem which is ideal for NP-hard problems.

Among the presented methods, SVM because of its simple structure has proper speed, but CNN, because of its deep structure, has long time consuming. Although, it has more precision than the SVM.[63]

A group also is the combination of the meta-heuristics and the ANNs which increases the complexity of the system and has not always the best result. In contrast, meta-heuristics are the algorithms that speed up the process of finding a promising suboptimal solution (eg, PSO, BBO, and WAO). The main advantage of the meta-heuristic methods is comparing to the aforementioned methods is their simplicity, although, they scarify the precision. Another advantage of the proposed system is because of using the chaos structure, its convergence speed is higher than most of the other complicated meta-heuristics.

For evaluating the performance of the proposed system, three evaluation function including correct detection rate (CDR), false acceptance rate (FAR), and false rejection rate (FRR) have been adopted.

CDR represents the fraction of the correctly classified pixels than all of the pixels and can be achieved as follows:

$$\mathrm{CDR} = \frac{\text{Number of pixels correctly classified as brain tumor}}{\text{Total pixels in the test dataset}}. \tag{19}$$

FAR determines the second parameter which shows the wrongly classified pixels that are not a brain tumor, but they have been classified in the tumor class than all of the pixels. The formula to find the FAR is given below:

$$\mathrm{FAR} = \frac{\text{Number of healthy pixels classified as tumor pixels}}{\text{Total pixels in the test dataset}}. \tag{20}$$

FRR is another evaluation function which determines the pixels which are a cancerous tumor but have been classified as healthy pixels than all of the pixels. This index is formulated below:

$$\mathrm{FRR} = \frac{\text{Number of tumor pixels classified as healthy pixels}}{\text{Total pixels in the test dataset}} \tag{21}$$

TABLE 3 Performance comparison of the presented method with other methods

Metric	SVM[58]	GA[31]	PSO[59]	NNPSO[59]	MLPPSOBBO[60]	CNN[61]	Proposed method
CDR (%)	83.8	84.3	84.8	84.3	85	86	**88**
FAR (%)	8.4	8.3	7.8	8.4	7.8	8	**10**
FRR (%)	7.8	7.3	7.3	7.3	7.2	6	**2**
MCC (%)	62.95	64.06	65.57	66.80	69.39	73.15	**76.83**

Note: The values in bold indicate that our proposed trick has better performace compared to SVM, GA, PSO, NNPSO, MLPPSOBBO and CNN.

Abbreviations: CDR, correct detection rate; CNN, ANN based on deep learning; FAR, false acceptance rate; FRR, false rejection rate; MCC, Matthews correlation coefficient; MLPPSOBBO, optimized ANN based on hybrid particle swarm optimization algorithm and biogeography-based optimization; NNPSO, particle swarm optimization-based ANN; PSO, particle swarm optimization; SVM, support vector machine.

TABLE 4 The average computation time for the proposed and state-of-the-art methods for 20 runs

Metric	SVM[58]	GA[31]	PSO[59]	NNPSO[59]	MLPPSOBBO[60]	CNN[61]	Proposed method
Time (seconds)	1.22	8.12	3.72	13.64	15.78	14.69	3.15

Abbreviations: CNN, ANN based on deep learning; MLPPSOBBO, optimized ANN based on hybrid particle swarm optimization algorithm and biogeography-based optimization; NNPSO, particle swarm optimization-based ANN; PSO, particle swarm optimization; SVM, support vector machine.

The performance of the proposed method is compared with that of the aforesaid methods and the results are given in Table 3.

Table 4 shows that using the presented algorithm in both feature selection and image classification improves the system performance as it overcomes the other existing methods for brain tumor detection.

In the following, the computational cost of the proposed method is evaluated. The way for dedicating the computational cost is to check the number of solutions that have been searched (calculated) and the associated computation time, that is, the more searched solutions and longer computation time, the higher the computational cost.

In the other side, however, small population size in meta-heuristics gives poor results; a large population size needs more computation time. So, to obtain a proper trade-off between these two features can help to improve the computational cost.

The advantage of the proposed CWAO uses the logistic map instead of the random numbers which improve its convergence speed and consequently decreases the computational cost.

Table 4 illustrates the average computation time for the proposed and state-of-the-art methods for 20 runs.

As can be seen, SVM because of its simple structure has the highest speed and among the meta-heuristics, after PSO algorithm which is famous for its speed, the proposed method has the highest speed. It should be noted that as declared before, in addition to speed, the system accuracy of the system is important for analyzing the computational cost.

9 | CONCLUSIONS

A brain tumor is a sign of the abnormal growth of cells in the human brain. Brain tumors can lead to cancer, which is one of the leading causes of death in the world. Early detection of tumors and estimation of their progress on the basis of MRI imaging help physicians to save lives. In this study, a general optimized system is presented for brain tumor detection. After applying image segmentation, 19 different features are extracted from the image. Afterward, an optimal feature selection based on the MCC and a newly developed optimization algorithm, CWAO is proposed. After feature selection, an optimized RBF network based on the introduced optimization algorithm is adopted for data classification into two classes of timorous and healthy. Three performance indexes have been employed for performance comparison of the proposed method toward state of the art methods.

10 | FUTURE RESEARCH DIRECTIONS

The proposed algorithm can be used to classify different kinds of cancers and medical images datasets. Another research area is to improve the optimization algorithm.[64-68] Using ANNs is also a promising method for improving the system efficiency, especially networks based on deep learning like convolutional neural networks. Another contribution can be the utilization of the evolutionary computation methods to speed up the fitness evaluation of neural networks for the process.

ACKNOWLEDGMENTS
The authors thank the organizers of ICO'2018, October 4 and 5, 2018, Hard Rock Hotel, Pattaya, Thailand, for the opportunity to presents their research results.

ORCID
Wei Gao https://orcid.org/0000-0001-7963-3502
Francis Abza https://orcid.org/0000-0001-8363-9341

REFERENCES

1. Liu J, Li M, Wang J, Wu F, Liu T, Pan Y. A survey of MRI-based brain tumor segmentation methods. *Tsinghua Sci Technol*. 2014;19(6):578-595.
2. Mohan G, Subashini MM. MRI based medical image analysis: Survey on brain tumor grade classification. *Biomed Signal Process Control*. 2018;39:139-161.
3. Bhattacharjee S, Ghatak S, Dutta S, Chatterjee B, Gupta M. A survey on comparison analysis between EEG signal and MRI for brain stroke detection. In: Abraham A, Dutta P, Mandal J, Bhattacharya A, Dutta S, eds. *Emerging Technologies in Data Mining and Information Security*. Berlin: Springer; 2019:377-382.
4. Saouli R, Akil M, Kachouri R. Fully automatic brain tumor segmentation using end-to-end incremental deep neural networks in MRI images. *Comput Methods Programs Biomed*. 2018;166:39-49.
5. Iqbal S, Ghani MU, Saba T, Rehman A. Brain tumor segmentation in multi-spectral MRI using convolutional neural networks (CNN). *Microsc Res Tech*. 2018;81(4):419-427.
6. Alhendawi KM, Al-Janabi AA, eds. An intelligent expert system for management information system failure diagnosis. *International Conference on Intelligent Computing & Optimization*. Berlin: Springer; 2018: 257-266.
7. Deepa B, Sumithra MG, Chandran V, Gnanaprakash V, eds. Fusion-Based Segmentation Technique for Improving the Diagnosis of MRI Brain Tumor in CAD Applications. *International Conference on ISMAC in Computational Vision and Bio-Engineering*. Berlin: Springer; 2018:299-307.
8. Liu Y, Wang W, Ghadimi N. Electricity load forecasting by an improved forecast engine for building level consumers. *Energy*. 2017;139:18-30.
9. Ahadi A, Ghadimi N, Mirabbasi D. Reliability assessment for components of large scale photovoltaic systems. *J Power Sources*. 2014;264:211-219.

10. Javadpour A, Mohammadi A. Improving brain magnetic resonance image (MRI) segmentation via a novel algorithm based on genetic and regional growth. *J Biomed Phys Eng*. 2016;6(2):95.
11. Razmjooy N, Mousavi BS, Soleymani F, Khotbesara MH. A computer-aided diagnosis system for malignant melanomas. *Neural Comput Applic*. 2013;23(7-8):2059-2071.
12. Rashid Sheykhahmad F, Razmjooy N, Ramezani M. A novel method for skin lesion segmentation. *Int J Inf Sec Sys Manage*. 2015;4(2):458-466.
13. Razmjooy N, Sheykhahmad FR, Ghadimi N. A hybrid neural network–world cup optimization algorithm for melanoma detection. *Open Med*. 2018;13(1):9-16.
14. Kosslyn SM. Images in the computer and images in the brain. *Comput Intell*. 1993;9(4):340-342.
15. Narayanan NH. Imagery: computational and cognitive perspectives. *Comput Intell*. 1993;9(4):303-308.
16. Kharma N, Mazhurin A, Saigol K, Sabahi F. Adaptable image segmentation via simple pixel classification. *Comput Intell*. 2018;34(2):734-762.
17. Ge Q, Xiao L, Wei ZH. Active contour model for simultaneous MR image segmentation and denoising. *Digi Signal Process*. 2013;23(4):1186-1196.
18. Corso JJ, Sharon E, Dube S, El-Saden S, Sinha U, Yuille A. Efficient multilevel brain tumor segmentation with integrated bayesian model classification. *IEEE Trans Med Imag*. 2008;27(5):629-640.
19. Ballanger B, Tremblay L, Sgambato-Faure V, et al. A multi-atlas based method for automated anatomical Macaca fascicularis brain MRI segmentation and PET kinetic extraction. *Neuroimage*. 2013;77:26-43.
20. Sarkar JP, Saha I, Maulik U. Rough possibilistic type-2 fuzzy C-means clustering for MR brain image segmentation. *Appl Soft Comput*. 2016;46:527-536.
21. Mahata N, Kahali S, Adhikari SK, Sing JK. Local contextual information and Gaussian function induced fuzzy clustering algorithm for brain MR image segmentation and intensity inhomogeneity estimation. *Appl Soft Comput*. 2018;68:586-596.
22. Mohsen H, El-Dahshan E-SA, El-Horbaty E-SM, Salem A-BM. Classification using deep learning neural networks for brain tumors. *Future Comput Inform J*. 2018;3(1):68-71.
23. Moallem P, Razmjooy N. A multi layer perceptron neural network trained by invasive weed optimization for potato color image segmentation. *Trends Appl Sci Res*. 2012;7(6):445.
24. Xia Y, Eberl S, Wen L, Fulham M, Feng DD. Dual-modality brain PET-CT image segmentation based on adaptive use of functional and anatomical information. *Comput Med Imag Graph*. 2012;36(1):47-53.
25. Maulik U. Medical image segmentation using genetic algorithms. *IEEE Trans Inf Technol Biomed*. 2009;13(2):166-173.
26. Moallem P, Razmjooy N, Ashourian M. Computer vision-based potato defect detection using neural networks and support vector machine. *Int J Robot Autom*. 2013;28(2):137-145.
27. Razmjooy N, Ramezani M. Training wavelet neural networks using hybrid particle swarm optimization and gravitational search algorithm for system identification. *Int. J. Mech. Electr. Comput. Sci*. 2016; 6(21):2987-2997.
28. Parsian A, Ramezani M, Ghadimi N. A hybrid neural network-gray wolf optimization algorithm for melanoma detection. *Biomed Res*. 2017;28(8):3408-3411.
29. Li Y, Jia F, Qin J. Brain tumor segmentation from multimodal magnetic resonance images via sparse representation. *Artif Intell Med*. 2016;73:1-13.
30. Zöllner FG, Emblem KE, Schad LR. SVM-based glioma grading: optimization by feature reduction analysis. *Z Med Phys*. 2012;22(3):205-214.
31. Kharrat A, Gasmi K, Messaoud MB, Benamrane N, Abid M. A hybrid approach for automatic classification of brain MRI using genetic algorithm and support vector machine. *Leonardo J Sci*. 2010;17(1):71-82.
32. Zeinalkhani L, Jamaat AA, Rostami K. Diagnosis of brain tumor using combination of K-means clustering and genetic algorithm. *Iran J Med Inform*. 2018;7:6.
33. Wang H, Fei B. A modified fuzzy C-means classification method using a multiscale diffusion filtering scheme. *Med Image Anal*. 2009;13(2):193-202.
34. Kekre H, Sarode T, Raut K. Detection of tumor in MRI using vector quantization segmentation. *Int J Eng Sci Technol*. 2010;2(8):3753-3757.
35. Kaur T, Saini BS, Gupta S. A novel feature selection method for brain tumor MR image classification based on the Fisher criterion and parameter-free Bat optimization. *Neural Comput Applic*. 2018;29(8):193-206.
36. Zhang Y, D-w G, Cheng J. Multi-objective particle swarm optimization approach for cost-based feature selection in classification. *IEEE/ACM Trans Comput Biol Bioinform*. 2017;14(1):64-75.

37. Emary E, Zawbaa HM, Grosan C, Hassenian AE, eds. Feature subset selection approach by gray-wolf optimization. *Afro-European Conference for Industrial Advancement*. Berlin: Springer; 2015:1-13.
38. Ghamisi P, Benediktsson JA. Feature selection based on hybridization of genetic algorithm and particle swarm optimization. *IEEE Geosci Remote Sens Lett*. 2015;12(2):309-313.
39. Lian C, Ruan S, Denœux T. An evidential classifier based on feature selection and two-step classification strategy. *Pattern Recogn*. 2015;48(7):2318-2327.
40. Razmjooy N, Mousavi BS, Sadeghi B, Khalilpour M, eds. Image thresholding optimization based on imperialist competitive algorithm. *3rd Iranian Conference on Electrical and Electronics Engineering (ICEEE2011)*. Qom, Iran: IEEE; 2011:1-10.
41. Clapham PJ. The humpback whale. *Cetacean Societies, field studies of dolphins and whales Chicago: The University of Chicago*. 2000;65(2):173-196.
42. Kaveh A, Ghazaan MI. Enhanced whale optimization algorithm for sizing optimization of skeletal structures. *Mech Based Des Struct Mac*. 2017;45(3):345-362.
43. Abdel-Basset M, El-Shahat D, El-henawy I. A modified hybrid whale optimization algorithm for the scheduling problem in multimedia data objects. *Concurr Comput Pract Exp*.e5137. http://doi.org/10.1002/cpe.5137.
44. Mafarja MM, Mirjalili S. Hybrid Whale Optimization Algorithm with simulated annealing for feature selection. *Neurocomputing*. 2017;260:302-312.
45. Oliva D, El Aziz MA, Hassanien AE. Parameter estimation of photovoltaic cells using an improved chaotic whale optimization algorithm. *Appl Energy*. 2017;200:141-154.
46. Wang J, Du P, Niu T, Yang W. A novel hybrid system based on a new proposed algorithm—multi-objective whale optimization algorithm for wind speed forecasting. *Appl Energy*. 2017;208:344-360.
47. Yang D, Li G, Cheng G. On the efficiency of chaos optimization algorithms for global optimization. *Chaos, Solit Fract*. 2007;34(4):1366-1375.
48. Rim C, Piao S, Li G, Pak U. A niching chaos optimization algorithm for multimodal optimization. *Soft Comput*. 2018;22(2):621-633.
49. Zhou M, Scott J, Chaudhury B, et al. Radiomics in brain tumor: image assessment, quantitative feature descriptors, and machine-learning approaches. *Am J Neuroradiol*. 2018;39(2):208-216.
50. Matthews BW. Comparison of the predicted and observed secondary structure of T4 phage lysozyme. *Biochim Biophys Acta Protein Struct*. 1975;405(2):442-451.
51. Hagh MT, Ghadimi N. Radial basis neural network based islanding detection in distributed generation. *Int J Eng Trans A Basic*. 2014;27:1061-1070.
52. Hagh MT, Ebrahimian H, Ghadimi N. Hybrid intelligent water drop bundled wavelet neural network to solve the islanding detection by inverter-based DG. *Front Energy*. 2015;9(1):75-90.
53. Mohammadi M, Talebpour F, Safaee E, Ghadimi N, Abedinia O. Small-scale building load forecast based on hybrid forecast engine. *Neural Process Lett*. 2018;48(1):329-351.
54. Noruzi A, Banki T, Abedinia O, Ghadimi N. A new method for probabilistic assessments in power systems, combining monte carlo and stochastic-algebraic methods. *Complexity*. 2015;21(2):100-110.
55. Eskandari Nasab M, Maleksaeedi I, Mohammadi M, Ghadimi N. A new multiobjective allocator of capacitor banks and distributed generations using a new investigated differential evolution. *Complexity*. 2014;19(5):40-54.
56. Vishnuvarthanan G, Rajasekaran MP, Vishnuvarthanan NA, Prasath TA, Kannan M. Tumor detection in T1, T2, FLAIR and MPR brain images using a combination of optimization and fuzzy clustering improved by seed-based region growing algorithm. *Int J Imag Syst Technol*. 2017;27(1):33-45.
57. Chui KT, DCL F, Lytras MD, Lam TM. Predicting at-risk university students in a virtual learning environment via a machine learning algorithm. *Comput Hum Behav*. 2018:105584.
58. Zhou J, Chan K, Chong V, Krishnan SM, eds. Extraction of brain tumor from MR images using one-class support vector machine. *2005 IEEE Engineering in Medicine and Biology 27th Annual Conference*. New York: IEEE; 2006:6-11.
59. Lahmiri S. Glioma detection based on multi-fractal features of segmented brain MRI by particle swarm optimization techniques. *Biomed Signal Process Control*. 2017;31:148-155.
60. Zhang Y, Wang S, Dong Z, Phillip P, Ji G, Yang J. Pathological brain detection in magnetic resonance imaging scanning by wavelet entropy and hybridization of biogeography-based optimization and particle swarm optimization. *Prog Electromagn Res*. 2015;152:41-58.

61. Havaei M, Davy A, Warde-Farley D, et al. Brain tumor segmentation with deep neural networks. *Med Image Anal*. 2017;35:18-31.
62. Liu RW, Ma Q, Yu SCH, Chui KT, Xiong N. Variational regularized tree-structured wavelet sparsity for CS-SENSE parallel imaging. *IEEE Access*. 2018;6:61050-61064.
63. Chui KT, Lytras MD. A novel MOGA-SVM multinomial classification for organ inflammation detection. *Appl Sci*. 2019;9(11):2284.
64. Ganesan T, Vasant P, Elamvazuthi I. *Advances in Metaheuristics: Applications in Engineering Systems*. Boca Raton: CRC Press; 2016.
65. Palestine I. An intelligent expert system for management information system failure diagnosis. *Intell Comput Optim*. 2018;866:257.
66. Vasant P, Kose U, Watada J. Metaheuristic techniques in enhancing the efficiency and performance of thermo-electric cooling devices. *Energies*. 2017;10(11):1703.
67. Zelinka I, Tomaszek L, Vasant P, Dao TT, Hoang DV. A novel approach on evolutionary dynamics analysis–a progress report. *J Comput Sci*. 2018;25:437-445.
68. Vasant P, Marmolejo JA, Litvinchev I, Aguilar RR. Nature-inspired meta-heuristics approaches for charging plug-in hybrid electric vehicle. *Wireless Netw*. 2019;1-14.

How to cite this article: Gong S, Gao W, Abza F. Brain tumor diagnosis based on artificial neural network and a chaos whale optimization algorithm. *Computational Intelligence*. 2019;1–17. https://doi.org/10.1111/coin.12259